An Adaptive Analog Circuit for LVDT's Nanometer Measurement Without Losing Sensitivity and Range

Gang Chen, Bo Zhang, Pinkuan Liu, and Han Ding, *Senior Member, IEEE*

Abstract—A self-adaptive circuit for the linear variable differential transformer (LVDT) has been developed to enhance its nanometer measurement range without loss resolution. By applying a fuzzy-proportional-integral-derivative controlled programmable gain amplifier array to produce a reference signal, which can adjust itself according to LVDT's core position, the conditioning circuit has ensured the signal to analog-to-digital converter varying in a very small interval over full-scale operating range. Thus, the sensitivity of the measurement system can be improved without losing measurement range. The simulation result demonstrated that the proposed circuit has solved the contradiction between resolution and range, which usually occurs in weak signal detection. Moreover, the signal-to-noise ratio has been ameliorated greatly. Additionally, the DSP-based signal conditioner, which utilizes the self-adaptive circuit, demonstrates the performance of the novel design and nanometer precision is obtained in a wide range.

Index Terms—Nanometer measurement, signal processing, programmable circuits, fuzzy control.

I. INTRODUCTION

LINEAR variable differential transformer (LVDT) has a widely applications in high accuracy measurement of position field [1], [2]. It can be used extensively for displacement measurement with a range of 1 mm to over 50 cm. Described in a patent by G.B. Hoadley in 1940, it became popular and plays a significant role in engineering and industries due to their ruggedness and high resolution [3]. Generally, LVDT consists of a single primary winding, two balanced secondary windings, a movable core, coil frame, shell and other components as illustrated in Fig. 1 [4]. When apply LVDT to practice field, the displacement of the movable core cannot exceed the linear range of the device.

The primary coil is excited by a sine wave with thousands Hz, and there is a phase difference between the primary and secondary signal. Based on whether or not use a center tap, LVDT can be generally classified into two classes,
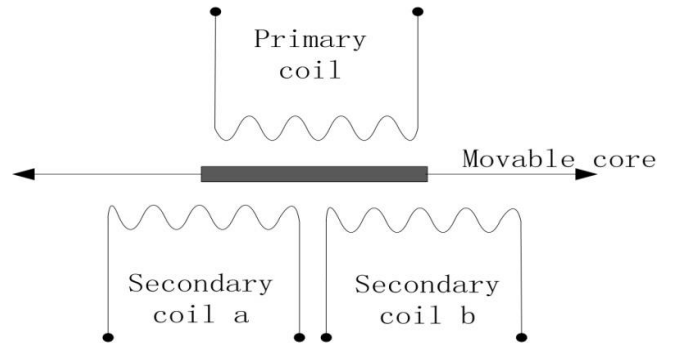
Fig. 1.   Schematic of LVDT.

namely the 4-wire and 5-wire scheme. The 5 wire scheme uses a center-tap to represent the connection point. The output signal from 5-wire LVDT's each secondary winding can be measured with respect to their connection point. On the contrary, the 4-wire LVDT do not have a center tap, and the output signal is the difference of the secondary coils.

The core displacement information, $A(x)$, can be analyzed as the baseband signal to be transmitted. By applying an excitation sine wave, $s(t) = A(x)\sin(2\pi f_0 t)$, a voltage is induced in the secondary winding. The difference between the two secondary voltages is linearly proportional to the core absolution position. Thus the idealism output can be described as follows [5]

$$U_o = A(x) \cdot \sin(2\pi f_0 t + \varphi) \tag{1}$$

Where A(x) depends on the LVDT core position, φ is the phase shift and f_o is the frequency of the excitation signal. This paper proceeds as follows: Section II reviews the state of the art LVDT conditioner and presents their problems. The schematic and the implementation process for single stage adaptive conditioning circuit is shown in section III. Section III also presents the multistage conditioning circuit which has increased the measurement range greatly. Section IV shows the simulation result of fuzzy-PID controller and compares the resolution & range curve of the novel and conventional method. The DSP-based signal conditioner with nanometer measurement precision in a wide range, which designed based on the self-adaptive circuit, was fabricated and shown in section IV. The conclusions are drawn in section V.

II. STATE OF THE ART LVDT CONDITIONING MODULES

The widely applications of LVDT have raised many researchers' attention to the development of LVDT's performances. Their work can be roughly classified into three categories.

A. The Reduction of Reading Uncertainty

When it comes to LVDT's signal conditioner, there are two available and well documented methods: the ratio-based method and the synchronous demodulation [6]. For the ratio-based method, the LVDT's position comes from the direct compute of the ratio of the LVDT secondary output and input primary excitation. However, as there is a phase lag in the secondary differential, the ratio based methods are inherently noisy and cannot achieve an accuracy measure of position. To address this problem, many researchers have introduced the phase compensation algorithm. Kumardeb Banerjee used a signal conditioner to locate the carrier peaks and provides a direct digital demodulation of the same at the said instants. Due to the peak sensitive demodulation is independent of the sensor induced phase lag and does not need any external phase compensation network, the FPGA-based LVDT signal conditioner has obtained a good performance [6].

The second method applied the standard phase-sensitive demodulation technique to the LVDT's secondary output, which is a double-sideband suppressed-carrier amplitude modulated (DSBSC-AM) waveform. Ralph M. Ford, et al [4] presented a DSP-based approach for a typical I/Q demodulator of LVDT signal conditioning. In their system, the position information is akin to the signal to be transmitted and the input sine wave excitation to the LVDT is akin to the carrier wave.

To address the long term stability and long distance reading, A. Masi, et al [5] presented a sine-fit algorithm digitally implemented on an FPGA. The proposed method has ensured high reading accuracy even with low signal-to-noise ratios. To improve the amplitude estimation of sinusoidal signals, Shang-The Wu and Jyun-Lang Hong [7] proposed a five-point amplitude estimation method. The five-point algorithm has achieved an estimation error less than 0.04%.

B. The Extending of Linearity Range and Calibration

Move the core toward any one of the secondary coils further, LVDT will show a nonlinearity behavior. This nonlinearity has limited the measurement range greatly and limited the application of LVDT, and a direct digital readout is not possible. Much effort has been made by researchers to deal with the nonlinearity characteristic of LVDT. By using a functional link artificial neural network, Saroj Kumar Mishra, et al [1] compensated the nonlinearity successfully. Sarita Das, et al [8] utilized a two-stage functional link artificial neural network (ANN) to enhance the linearity and improved the accuracy and precision of LVDT to some extent. The ANN also used by Santhosh K.V. [9] to extend linearity range of the overall system. Moreover, the application of ANN in Santhosh's paper makes the system independent of physical parameters of LVDT. To calibrate the LVDT and address the nonlinearity, Jong-Kyoung Lee, et al [10] employed an additional secondary coil and new signal processing method to calibrate the sensitivity variation. Hyo-moon Cho, et al [11] proposed a signal mapping based algorithm to calibrate the LVDT and reduced the time of calibration process greatly. Robert S. Weissbanch, et al [12] tested and compared the LVDT signal demodulator. The results showed that the DSP based conditioner shared a better linearity than the AD598 and SE-based signal conditioners, and matches the linearity of the AD698.

C. Rejection of Magnetic Variation

Static or slowly varying magnetic fields can induce a position reading drift and affect the performances of LVDT greatly. To address this problem, many researchers try to offer a quantitative information on the induced error. Many of them are based on the analysis of FEM modeling and experimental measurement. Alessandro Masi, et al [13] presented an LVDT finite element model and its experimental validation. Their study had offered a tool to investigate the effects of external magnetic fields on LVDTs and how to design of less sensitive devices. Michele Maritno, et al [14] introduced an analytical model to describe the effects of an external DC magnetic field on the harmonics amplitude of the secondary voltages of the LVDT. Their works had shown the sensor's geometry and its materials can affect the performance of LVDT and proposed the concept of equivalent differential permeability.

The literatures reviewed above covered the issues about the LVDT's accuracy, immune to environmental variation and ability to resolve position down to the atomic scale. When it comes to LVDT's large range nanometer measurement ability, however, the problem is barely addressed before, and no LVDT signal conditioner can provide a solution for large range nanometer measurement.

Moreover, the random noise of the LVDT causes an uncertainty in the measured result which also affect the performance greatly. The mistake will occur if the distance between two measured locations is smaller than the uncertainty. Since the noise is random, to specify a resolution where adjacent locations never overlap will be impractical. To address this problem, the probability that the measured value is within a certain error bound is used. The 6σ-resolution can be described as a function of the bandwidth f_h, noise density $\sqrt{A}$, and 1/f corner frequency f_{nc} [3],

$$6\sigma - resolution = 6\sqrt{A}\sqrt{f_{nc}\ln\frac{f_h}{f_l} + k_e f_h} \qquad (2)$$

Equation (2) indicates that the resolution is approximately proportional to the square-root of bandwidth when fh≫fnc. Limited by the Johnson shoes and Barkhausen noise, the theoretical resolution of the LVDT sensor has a limited resolution. However, standard conditioning circuits such as the AD598, its maximum resolution is approximately 5 nm with a 1kHz bandwidth only in a range of 0.5mm when with a driving amplitude of 5Vp-p. Take the above discussion into consideration, we can see that the conventional LVDT's signal conditioner cannot achieve a high resolution in a large range for two main reasons: the sensitivity cannot be improved due to the limited driving amplitude, the signal to noise ratio has not been improved as the noise density has not been reduced.

III. THE PROPOSED METHOD

To solve these problems and design a signal conditioner for LVDT's Nanopositioning without losing range, a fuzzy-PID
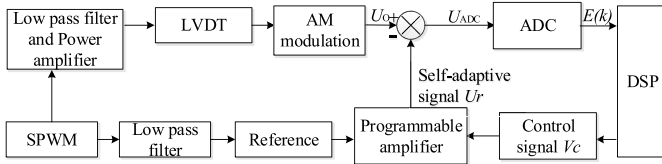
Fig. 2.   Block diagram of the single stage conditioning circuit.

Fig. 3.   The block diagram of fuzzy-PID controller.

controlled adaptive circuit was proposed in this paper. In the proposed signal conditioner system, a programmable amplifier was utilized, whose controlling signal came from the output of the fuzzy-PID controller. The novel circuit can be programmed to meet the dynamic demand of a measurement system. For a single phase programmable circuit, it consists of an ADC, a digital to analog converter (DAC), a programmable gain amplifier (PGA), a DSPF2812 chip and some other interface circuit which are shown in Fig. 2. In many applications, the PGA is used to amplify the signal to ADC to verify the signal matching the requirement of the input signal of ADC. However, to guarantee the measurement range, the scale-up factor is limited which leads to the loss of sensitivity. To solve this problem, in the proposed circuit, the PGA is used to amplify the reference signal adaptively, while the ADC's input signal comes from a different circuit. By adjusting the magnification of the reference signal automatically according to the sensor's output signal, the signal to ADC is limited in a small interval that almost close to zero. In this way, the sensitive of the senor has been guaranteed in a high level without loss range.

The main role of the conditioning circuit is to adjust the reference signal's amplitude to make the LVDT's output signal match the ADC's input requirement over full-scale operating range. In this system, the LVDT was excited by a sine signal generated by the DSP's SPWM signal [15].

The reference signal also comes from PWM module, simultaneously. A low pass filter and a phase adjustment circuit were employed to ensure the same phase of reference and LVDT's output signal. Let U_r be the reference signal, then

$$U_r = K(x) \cdot \sin(2\pi f_0 t + \varphi) \tag{3}$$

The signal to ADC, U_{ADC}, can be rewriter as follows:

$$\begin{aligned} U_{ADC} &= U_o - U_r + 1.5 \\ &= (A(x) - K(x)) \sin(2\pi f_0 t + \phi) + 1.5 \end{aligned} \tag{4}$$

Where: $K(x)$ is the PGA's gain which controlled by a voltage signal comes from the DAC module; 1.5 is the DC bias. Here the VCA810 was chosen as the PGA chip which is a voltage control PGA. Let V_c be the controlling signal, the transform function is the following equation.

$$K(x) = 10^{-2(V_c(x)+1)} \tag{5}$$

Compared with the conventional design, from Fig. 2 we can see the novel method has some good features as follows: first, as the signal to the ADC is controlled in a small interval, the gain of the LVDT's output can be high, thus the sensitive can be guaranteed; Second, due to the structure of the DAC, the error of the output of the DAC is a fixed factor and can be eliminated when calibrates the output signal, then the output
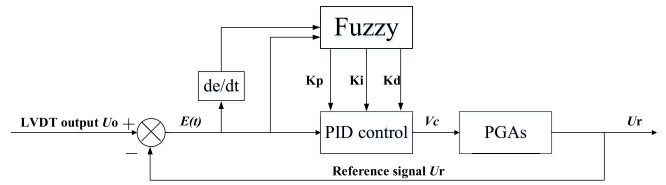
of DAC can be controlled precisely. Thus the resolution of the signal conditioner is mainly restricted by the noise that contained in the signal and freed from the resolution of the DAC and ADC.

A. Gain Setting Strategy for Single Stage Circuit

In this system, both the ADC and DAC have 14-bit resolution. In order to obtain a nanometer measurement resolution, the scale factor of the LVDT's output signal must be chosen adaptively.

Define u^+ as the saturation of the operational amplifier which also the maximum output signal of the LVDT and d as the maximum range of the core. In this case, $u^+ = 15V$, $d = \pm 500um$, $U_{ADC} < 3V$, then the measurement resolution can be rewritten as

$$\delta = \frac{d \cdot U_{ADC}}{2 \cdot 2^{14} \cdot u^+} \approx 5nm \tag{6}$$

To guarantee the full scale measurement, the signal U_{ADC} should vary in a small interval, and the best situation is $U_{ADC} = 1.5V$. Then

$$(A(x) - K(x)) \sin(2\pi f_0 t + \phi) = 0 \tag{7}$$

The adaptive adjusting the gain $K(x)$ based on the LVDT's output signal is a control problem. While the proportional-integral-derivative (PID) control is probably the most widely used control strategy in feedback control design owing to its simplicity and good dynamical and robustness properties [16]. The typical PID control law in its standard form is

$$V_c(k) = K_p e(k) + K_i \sum_{j=0}^{j=k} e(j) + K_d[e(k) - e(k-1)] \tag{8}$$

Where Kp, Ki and Kd denote the proportional, integral, and derivative gain, and $e(k)$ is the difference between ADC sampling result and 1.5.

Taking the complexity of the dynamic measurement process into consideration, freedom to select the proportional, integral, and derivative gain will be of worth in real applications. For these reasons, it is highly befitting to increase the capabilities of PID controllers by adding new features to typical PID [17]. In this paper, the fuzzy logic seems to be a particularly appropriate choice since it allows us to exploit the field application experience and therefore add some sort of intelligence to the automatic control system [18]. The block diagram of the control system is shown in Fig. 3. The system's mathematical model can be described as
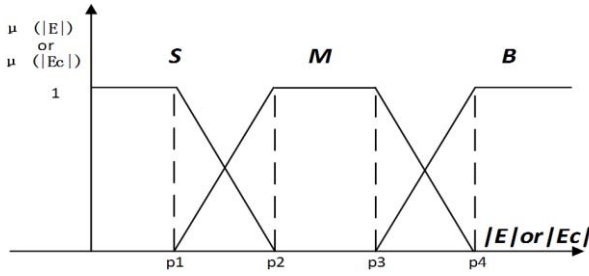
$$G(s) = \frac{0.0015e^{-0.0002s}}{s + 4.6} \tag{9}$$

Fig. 4. The membership function of |E| and |Ec|.

TABLE I
THE PARAMETERS OF FUZZY PID FOR EACH RULE

Kp	K_{p1}	K_{p2}	K_{p3}	K_{p4}	K_{p5}
	8e6	6.6e6	4.4e6	4.4e6	4.4e6
Ki	K_{i1}	K_{i2}	K_{i3}	K_{i4}	K_{i5}
	0	0	0	1.5e8	4.5e8
Kd	K_{d1}	K_{d2}	K_{d3}	K_{d4}	K_{d5}
	0	100	200	200	400

Fig. 5. Unit step response of the traditional PID and Fuzzy PID.
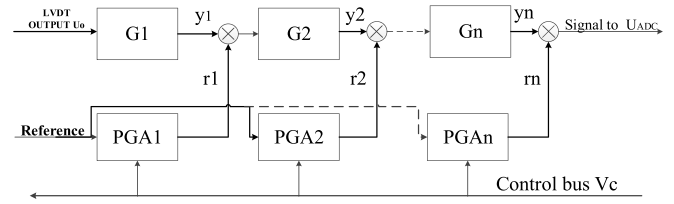
Fig. 6. Block diagram of the multistage conditioning circuit.

Taking the real-time implementation of the fuzzy self-tuning (FLT) algorithm into consideration, an approach to design the FLT has been adopted in [19]. In this case, the input vector of the fuzzy-PID controller will be the absolute value of error and error's derivative. That is |E| and |Ec|, the membership function is shown in Fig. 4.

The universe of discourse of |E| and |Ec| goes from 0 to a maximum value of the input variable |E|max and |Ec|max. Here partitioned the input variable into three fuzzy sets: B (big), M (medium), and S (small) with each attribute is described by the membership function which showed in Fig. 3

A fuzzy rule based for the case of this FLT with two input variable and one output vector is given by the general canonical IF-THEN rule for

$$if \ |E| \ is \ A^l \ and \ |Ec| \ is \ B^l, \ then \ Y \ is \ C^l$$

Where Al, Bl and Cl are fuzzy sets and $l = 1, \ldots, m$ is the number of rules. After the analysis of the control plant and combined with practical experiment, to simplify the control process, here we only used five rules for this case as follows.

if |E| is B, then $K_p = K_{p1}, K_i = K_{i1}, K_d = K_{d1}$;
if |E| is M and |Ec| is B,
then $K_p = K_{p2}, K_i = K_{i2}, K_d = K_{d2}$;
if |E| is M and |Ec| is M,
then $K_p = K_{p3}, K_i = K_{i3}, K_d = K_{d3}$;
if |E| is M and |Ec| is S,
then $K_p = K_{p4}, K_i = K_{i4}, K_d = K_{d4}$;
if |E| is S, then $K_p = K_{p5}, K_i = K_{i5}, K_d = K_{d5}$

Where Kp1~Kp5, Ki1~Ki5 and Kd1~Kd5 is the tuning result that combined with practical experience for the parameter of the PID controller for each state which showed in Table I.

The comparison of the traditional PID and Fuzzy-PID's unit step response is shown in Fig. 5, even though the Fuzzy PID only has five rulers which limited by the computation, the unit step response is much better than the traditional PID.
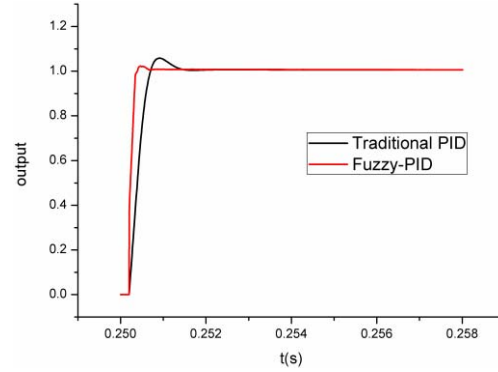
B. Improvement in Range and Multistage Circuit

The fuzzy-PID controller shown above makes the signal to the ADC fluctuate in a small span wherever the core is, which guarantees the input signal to ADC always under saturation. Therefore, when the novel conditioning circuit has a fixed resolution, then the displacement range for the core is only limited by the saturation voltage of the PGA and the integrated operational amplifier used in the conditioning circuit. For a single-stage conditioning circuit, we will have

$$\frac{L_n}{L_c} = \frac{u^+}{1.5} \tag{10}$$

Where Ln denotes the range of the novel method and Lc denotes the conventional method, and u^+ is the saturation voltage of PGA and integrated operational amplifier. Assume that $u^+ = 15V$, according to (9), the range has increased to 10 times than the conventional design.

The single stage conditioning circuit's range is limited by the saturation voltage of the amplifier, while if split the conditioning circuit in several stages, which shown in Fig. 6, the range can be extended to a very large scale.

When it comes to multistage conditioning case, the PGAA's Gain setting strategy is another problem should be resolved. If every PGA has its own fuzzy-PID controller, the computation will be beyond the CPU's load which makes it impossible to realize real-time measurement. What's more, if every PGA works at its own optimal gain, a small noise will lead to system oscillations. That is to say, the system's anti-jamming capability will be reduced.

The multistage gain programmable setting strategy used in this paper is simple and efficient. The PGA closed to ADC is controlled by the fuzzy PID algorithm, while the other PGAs' gain are updated according to the controlled PGA. Based on the controlled PGA, other PGAs can self-adapt itself to work in an unsaturation state. In this case, the block diagram of the control system is shown in Fig. 7.
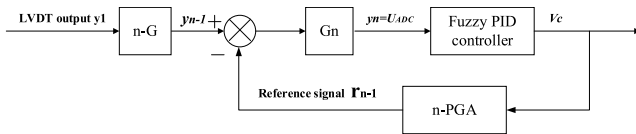
Fig. 7.   The block diagram of multistage controller.

Fig. 8.   Simulation result of the conditioning circuit.

To simplify the computation and the complexity of the hardware system, the operation amplifies' gain for the LVDT's output signal is the same. And the PGAs' gain are also the same and controlled by the fuzzy-PID controller. Let G_n is the gain of the nth operation amplifier and $G_n = \lambda$. Then we have

$$G_1 = G_2 = \cdots\cdots = G_n = \lambda \tag{11}$$

Let y_n be the output signal's amplitude from the nth operation amplifier, and r_n is the reference signal's amplitude from nth PGA. According to Fig. 6 we have

$$y_n = (y_{n-1} - r_{n-1}) \cdot G_n \tag{12}$$

As $r_n = r_{n-1} = r_{n-1} = \cdots\cdots = r_1 = \eta$, then

$$y_n = \lambda^{n-1} y_1 - \sum_{i=1}^{n-1} \lambda^i \cdot \eta \tag{13}$$

If the number of stages is n, which means $y_n = U_{ADC}$. Then the block diagram can be described as follows:

From the block diagram of the controller, we can see the update of PGAs can be gotten as

$$\Delta Vc(k) = H(k) \cdot \Delta U_{ADC}(k) = H(k) \cdot [y_n(k) - y_n(k-1)] \tag{14}$$

Where H(k) is the transfer function of the controller at time k.

For the multistage circuit, when all the PGAs' output signal reach to its saturation output, the idealized measurement range can be expressed as

$$\frac{L_n{}'}{L_c} = \frac{Nu^+}{1.5} \tag{15}$$

Equation (15) shows that the proposed method has the ability to obtain a very large measurement range if we ignore the electronic noise introduced by the adaptive circuit. Because when N is increased, the range will be enhanced simultaneously. However, in practice, noise is a fact that affects the performance of the device and cannot overpass. Thus much attention should be paid to the suppression of noise.

C. Improvement in SNR

The signal comes from LVDT consist of two parts, one part from the ADC and another from the reference signal. For a single stage conditioning circuit, the output signal can be written as

$$U_o = U_{ADC} + U_r = s_{ADC} + n_{ADC} + s_r + n_r \tag{16}$$

Where s_{ADC} denotes the useful signal from ADC and n_{ADC} denotes the noise from ADC [20]; s_r denotes the useful signal from the reference signal and n_r denotes the noise in reference.
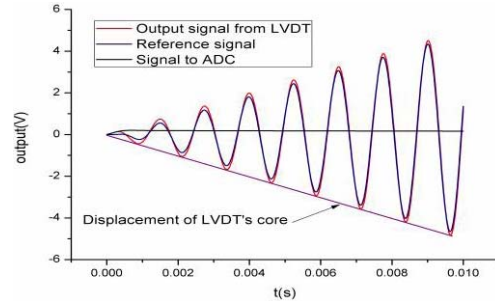
As the reference signal is stable and unchanged, the signal's spectrum can be analyzed very clearly. In this way the useful signal can be extracted and the noise can be eliminated. Assume that the original signal's signal to noise ratio is χ, then (16) can be rewritten as

$$U_o = s_{ADC}(1 + \chi) + s_r \tag{17}$$

And the SNR for the novel design can be expressed as

$$SNR = \frac{s_{ADC} + s_r}{\chi s_{ADC}} \tag{18}$$

For the conventional conditioning circuit

$$SNR' = \frac{1}{\chi} \tag{19}$$

Then we have

$$\zeta = \frac{SNR}{SNR'} = 1 + \frac{s_r}{s_{ADC}} \tag{20}$$

As the signal to ADC is controlled by the fuzzy-PID controller, owing to the noise and DSP's limited performance, the s_{ADC} cannot be limited near zero, according to the simulation result, $s_{ADC} = 0.2V$, that is to say, the SNR has been improved to about 75 times.

IV. SIMULATION AND APPLICATION

The pivotal idea of the novel conditioning circuit is using a reference signal minus the original signal to guarantee the signal to ADC changing in a small interval. The self-adaptive strategy is realized by the fuzzy PID controller. In order to observe the conditioning circuit's performance, a simulation which based on Matlab was conducted. In the simulation system, the excitation signal for LVDT is 7 kHz, and the core's displacement increases linearly. Fig. 8 illuminates that the reference signal can adjust itself in line with the LVDT's output signal which is the red and blue curves. The black curve in Fig. 8 which changed in a small span is the signal to the ADC. The result also shows that the signal to the ADC is not as we expected near zero, that because the controller's delay effect.

To verify the practical feasibility of the novel method, an experiment platform was built which showed in Fig. 9, a nano-position platform was applied to drive LVDT's core and calibrate the measurement system which has a resolution of 0.3nm. The DSP system produced the PWM signal and processed the digital signal from the conditioning circuit simultaneously. The conditioning circuit in the picture is a
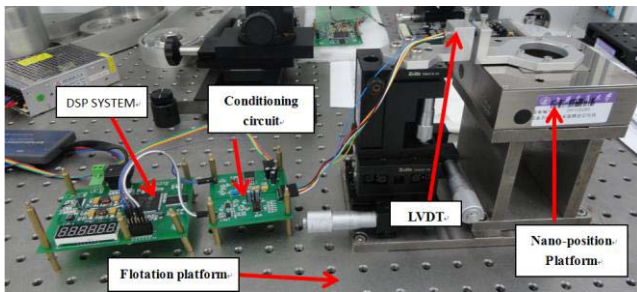
Fig. 9. The experimental platform for the novel method.

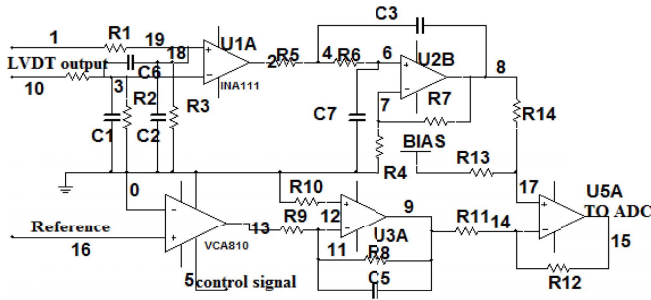Fig. 11. Comparison of resolution against range curve.

Fig. 10. Self-adaptive circuit of single stage.

single stage self-adaptive circuit whose circuit schematic is shown in Fig. 10.

To see the difference in performance between the novel and conventional method, a comparative test was conducted. In the experiment, an error compensation polynomial was used to solve the error of the LVDT's nanometer measurement. For the conventional method, there isn't a self-adaptive reference signal for the measurement system, to make this happen, the controlling signal for the programmable amplifier is fixed. Afterward, via changing the scale factor of the LVDT's output signal, the relationship between resolution and range was demonstrated. As the signal to the ADC's amplitude is limited by the saturation voltage, during the test, it is very clear that the larger scale factor, the smaller range will be. To test the performance of the novel method, the scale factor for LVDT's output signal was fixed at a high level, and the self-adaptive circuit is enabled. Through changing the displacement of the core to see the signal to ADC's voltage level, we got the relationship between resolution and range for the novel method which showed in Fig. 11. From the comparison of the resolution against range curve in Fig. 11, the black curve demonstrated the conventional method can't provide a high resolution and large range simultaneously. The red curve showed the novel method, however, has solved this contradiction.

V. CONCLUSION

A self-adaptive circuit for LVDT's large range nanometer measurement was presented. Compared to the SE-based, DSP-based, and AD598 based method, the proposed circuit utilizes a reference signal to enhance the measurement resolution and range simultaneously. The proposed method has avoided the restrict factor of ADC's saturation, made the
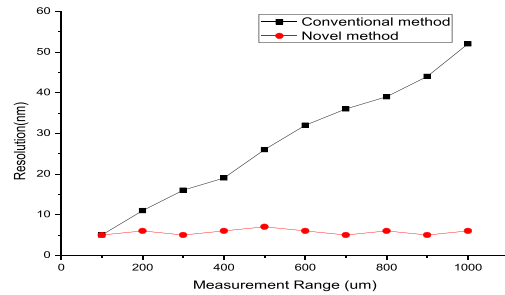
sensitivity and range be free variables in designing measurement system.
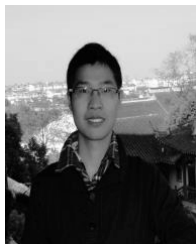
To demonstrate the feasibility of the novel method, a simulation based on Matlab was conducted and the result showed the good performance of fuzzy-PID controller. To test the performance in reality, an experiment platform was built which included the floating platform, nano-positioning platform, DSP system and so on. The experiment result showed the proposed method had achieved nanometer resolution measurement in a large range. Even though the experiment just achieved 5nm measurement, but via the simulation, we could obtain a higher resolution and larger range by applying multistage self-adaptive circuit and advanced noise restriction methodology.

The proposed circuit is designed for LVDT but it is not limited to this case, as in weak signal detection field, the designers are always faced with the contradiction between range and sensitivity. Hence, the proposed circuit will come into power in all weak signal detection fields.

REFERENCES

[1] S. K. Mishra, G. Panda, and D. P. Das, "A novel method of extending the linearity range of linear variable differential transformer using artificial neural network," *IEEE Trans. Instrum. Meas.*, vol. 59, no. 4, pp. 947–953, Apr. 2010.

[2] D. Trapani, N. Biasi, M. De Cecco, and D. Zonta, "Validation of MEMS acceleration measurements for seismic monitoring with LVDT and vision system," in *Proc. IEEE Workshop Environ. Energy Struct. Monitor. Syst. (EESMS)*, Sep. 2012, pp. 104–109.

[3] A. J. Fleming, "A review of nanometer resolution position sensors: Operation and performance," *Sens. Actuators A, Phys.*, vol. 190, pp. 106–126, Feb. 2013.

[4] R. M. Ford, R. S. Weissbach, and D. R. Loker, "A novel DSP-based LVDT signal conditioner," *IEEE Trans. Instrum. Meas.*, vol. 50, no. 3, pp. 768–773, Jun. 2001.

[5] A. Masi, S. Danzeca, R. Losito, P. Peronnard, R. Secondo, and G. Spiezia, "A high precision radiation-tolerant LVDT conditioning module," *Nucl. Instrum. Methods Phys. Res. Sec. A, Accel., Spectrometers, Detectors Assoc. Equip.*, vol. 745, pp. 73–81, May 2014.

[6] K. Banerjee, B. Dam, and K. Majumdar, "A novel FPGA-based LVDT signal conditioner," in *Proc. IEEE Int. Symp. Ind. Electron. (ISIE)*, May 2013, pp. 1–6.

[7] S.-T. Wu and J.-L. Hong, "Five-point amplitude estimation of sinusoidal signals: With application to LVDT signal conditioning," *IEEE Trans. Instrum. Meas.*, vol. 59, no. 3, pp. 623–630, Mar. 2010.

[8] S. Das, D. P. Das, and S. K. Behera, "Enhancing the linearity of LVDT by two-stage functional link artificial neural network with high accuracy and precision," in *Proc. 8th IEEE Conf. Ind. Electron. Appl. (ICIEA)*, Jun. 2013, pp. 1358–1363.

[9] K. V. Santhosh and B. K. Roy, "A smart displacement measuring technique using linear variable displacement transducer," *Proc. Technol.*, vol. 4, pp. 854–861, 2012.

[10] J.-K. Lee, Y.-H. Ko, and S.-G. Lee, "Calibration technique for sensitivity variation in RVDT type accelerator position sensor," in *Proc. IEEE Int. Instrum. Meas. Technol. Conf. (I2MTC)*, May 2013, pp. 1512–1516.

[11] H.-M. Cho, J.-H. Son, and J.-H. Lee, "A novel signal-mapping based LVDT signal conditioner," in *Advances in Electrical Engineering and Electrical Machines*. New York, NY, USA: Springer, 2011, pp. 453–461.

[12] R. S. Weissbach, D. R. Loker, and R. M. Ford, "Test and comparison of LVDT signal conditioner performance," in *Proc. 17th IEEE Instrum. Meas. Technol. Conf. (IMTC)*, May 2000, pp. 1143–1146.

[13] A. Masi, A. Danisi, R. Losito, M. Martino, and G. Spiezia, "Study of magnetic interference on an LVDT: FEM modeling and experimental measurements," *J. Sensors*, vol. 2011, no. 5294545, pp. 1–9, Apr. 2011.

[14] M. Martino, G. Golluccio, R. Losito, and A. Masi, "An analytical model of the effect of external DC magnetic fields on the AC voltages of an LVDT," in *Proc. IEEE Instrum. Meas. Technol. Conf. (I2MTC)*, May 2010, pp. 213–218.

[15] F. J. Wu, B. Sun, and H. R. Peng, "Single-phase three-level SPWM scheme suitable for implementation with DSP," *Electron. Lett.*, vol. 47, no. 17, pp. 994–996, Aug. 2011.

[16] C. F. de Paula and L. H. Ferreira, "An improved analytical PID controller design for non-monotonic phase LTI systems," *IEEE Trans. Control Syst. Technol.*, vol. 20, no. 5, pp. 1328–1333, Sep. 2012.

[17] I. Pan, S. Das, and A. Gupta, "Tuning of an optimal fuzzy PID controller with stochastic algorithms for networked control systems with random time delay," *ISA Trans.*, vol. 50, no. 1, pp. 28–36, 2011.

[18] B. Zhang, W. X. Zheng, and S. Xu, "Passivity analysis and passive control of fuzzy systems with time-varying delays," *Fuzzy Sets Syst.*, vol. 174, no. 1, pp. 83–98, 2011.

[19] J. L. Meza, V. Santibáñez, R. Soto, and M. A. Llama, "Fuzzy self-tuning PID semiglobal regulator for robot manipulators," *IEEE Trans. Ind. Electron.*, vol. 59, no. 6, pp. 2709–2717, Jun. 2012.

[20] A. Sanginario, M. Giorcelli, A. Tagliaferro, and D. Demarchi, "Improving the signal-to-noise ratio of an ECL-based sensor using ad hoc carbon nanotube electrodes," *J. Micromech. Microeng.*, vol. 22, no. 7, p. 074010, 2012.

Bo Zhang received the B.E. and M.E. degrees from Northwestern Polytechnical University, Xi'an, China, in 2000 and 2003, respectively, and the Ph.D. degree from the School of Mechanical Engineering, Shanghai Jiao Tong University (SJTU), Shanghai, China, in 2008.

He is currently with the Research Institute of Robotics, SJTU. His research interests include nanopositioning, micromanipulation, smart actuators and sensors, and precision parallel robots.

Pinkuan Liu was born in Hubei, China, in 1969. He received the B.S. degree in precision machine and instrument engineering, and the M.S. and Ph.D. degrees in mechatronic engineering from the Harbin Institute of Technology (HIT), Harbin, China, in 1991, 1998, and 2003, respectively.

He was with the Robotics Institute, HIT, from 1998 to 2003, where he was appointed as an Associate Professor in 2002. From 2003 to 2005, he was a Post-Doctoral Fellow with the Institute of Machine and Production Engineering, Technical University of Braunschweig, Braunschweig, Germany. He joined Shanghai Jiao Tong University, Shanghai, China, in 2005, where he is currently with the Research Institute of Robotics. His research interests include nanopositioning, micro-manipulation, smart actuators and sensors, and precision parallel robots.

Gang Chen received the B.S. degree in mechanical engineering from Shanghai Jiao Tong University, Shanghai, China, in 2012, where he is currently pursuing the M.S. degree at the School of Mechanical Engineering.

His research interests include signal processing, machine fault diagnosis, robotics, and machine learning.

Han Ding (M'97–SM'00) received the Ph.D. degree from the Huazhong University of Science and Technology, Wuhan, China, in 1989.

He is currently a Cheung Kong Chair Professor with Shanghai Jiao Tong University, Shanghai, China. His research interests include robotics and multiaxis machining.

Dr. Ding is a Technical Editor of the IEEE/ASME TRANSACTIONS ON MECHATRONICS. He serves as a Guest Editor and Technical Committee Member for semiconductor manufacturing automation of the IEEE Robotics and Automation Society. He has organized and chaired many technical sessions and workshops of various international conferences.